In-situ stress-strain measurement of bridgmanite

*Noriyoshi Tsujino[1], Daisuke Yamazaki[1], Moe Sakurai[1], Fang XU[1], Yuji Higo[2]

1. Institute for Planetary Materials, Okayama University, 2. Japan Synchrotron Radiation Research Institute

In order to understand mantle dynamics in the Earth’ s interior, it is important to know the viscosity of the Earth’ s lower mantle. One dimensional viscosity models of the Earth’ s mantle were proposed by geophysical observations while there are large inconsistencies of viscosity (2~3 order magnitude) in the lower mantle between suggested models. Therefore it is important to determine viscosity of lower mantle minerals by high pressure experiments in order to understand mantle dynamics. In this study, we conducted in-situ stress-strain measurements of bridgmanite aggregate using Deformation-DIA type apparatus as Kawai-type.
In-situ measurements were conducted using SPEED-Mk.II, which is D-DIA apparatus, as Kawai-type apparatus at SPring-8 BL04B1. Mg-pure bridgmanite aggregates were used as starting material. Experimental conditions are 1473-1673 K and 27-28 GPa. Pressures were estimated by equation of state on bridgmanite (Katsura et al., 2009). WC second cubic anvils with slit or cone (5˚) to take tomography and 2D X-ray diffraction, was used along X-ray path. X-ray radiographies of the strain markers were taken using an imaging system composed of a YAG crystal and a CCD camera. Two-dimensional X-ray diffraction patterns were corrected for 180-300 s using CCD detector. To calculate pressure and the stress magnitude of bridgmanite, (111) (112) (200) X-ray diffraction peaks were used.
Measured uniaxial stress and strain of bridgmanite during deformation experiments were 0.3-1.3 GPa and < 6 %. Flow law in dislocation creep is described by,
$d\varepsilon/dt = A\sigma^3 \exp(-E^*/RT)$ (1)
where $d\varepsilon/dt$ is strain rate, A is pre-exponent, σ is stress, E^* is activation energy, R is gas constant and T is temperature. Least squares fit of Eq. (1) to these viscosity data yielded $A = 10^{7.6\pm1.5}$ and $E^* = 372 \pm 40$ kJ/mol. This activation energy of flow low is similar to that of atomic diffusion of bridgmanite by Xu et al. (2011). This fact supported deformation mechanism could be dislocation creep controlled by dislocation clime.

Keywords: bridgmanite, lower mantle, In-situ measurements, viscosity

Diffusion creep and grain growth in forsterite + 15vol% enstatite aggregate

*Tadashi Nakakoji[1], Takehiko Hiraga[1], Hiromichi Nagao[1], Shin'ichi Ito[1], Masayuki Kano[1]

1. Earthquake Research Institute, The Univeristy of Tokyo

In this study, we conducted grain growth and creep experiments on the same fine-grained forsterite + 15vol% enstatite aggregate under high temperature. We rapidly changed load applying to the sample for “stepped test”, which was aimed to infer creep mechanisms at a wide range of stress. We gradually changed temperature under application of a constant load for “gradual temperature change test” to collect vast numbers of stress/strain rate/grain-size/temperature data which allow their statistical analyses to obtain precise flow parameters such as pre-exponential factors and activation energies for given flow laws. Grain growth experiment with a long duration (= 500 h) at different temperatures was aimed to obtain a precise temperature dependency of grain growth. Dependency of *n* on stress was investigated from the results of stepped tests conducted at temperatures from 1150˚C to 1370˚C at stress ranging from 5 MPa to 300 MPa. We found monotonic decrease of stress exponent from 2 to 1 with increasing stress and its rapid increase to > 3 at high stress regime. We inferred that interface-reaction control diffusional creep and grain boundary (GB) diffusion creep worked sequentially at low stress, while GB diffusion creep and dislocation creep worked parallel at high stress condition. Activation energy of 432 kJ/mol for GB creep and pre-exponential factor of 6.15×10^{11} $um^3K/MPa/sec$ were obtained from MCMC analyses mainly of the results of gradual temperature change tests. Grain growth experiment showed a monotonic increase in grains size of both forsterite and enstatite phases with increasing temperature at > 1300˚C.
Diffusivities estimated from creep and grain growth rates using classic GB diffusion creep and grain growth laws well coincide at all experimental ranges indicating that governing diffusional processes for creep and grain growth are identical. We compare our obtained diffusivities with the results of previous direct measurements on grain boundary self-diffusivities of MgO (*Gardes and Heinrich*, 2011) and Si (*Fei et al.*, 2016) finding that MgO GB diffusion rather than Si explains our observations.

Keywords: upper mantle rheology, grain growth, diffusion creep, olivine, diffusivity, rate-controlling element

Creep behavior and high-pressure faulting during the olivine-spinel transformation in fayalite

*Tomoaki Kubo[1], Naoko Doi[1], Masahiro Imamura[1], Takumi Kato[1], Yuji Higo[2], Yoshinori Tange[2]

1. Kyushu University, 2. JASRI

Transformations from metastable olivine at large overpressures in cold subducting slabs may cause significant grain-size reduction and lead to the slab weakening and deep earthquakes. It is indispensable to investigate the coupling process between transformation and deformation under pressures of mantle transition zone. In the present study, we examined creep behaviors during the olivine-spinel transformation in fayalite (Fe_2SiO_4) up to ~14 GPa and observed some evidences for transformational faulting. Deformation experiments were conducted using a Deformation-DIA apparatus in the beamline of BL04B1 at SPring-8. After annealing polycrystalline fayalite at ~3.5 GPa and 900˚C for 2 h, we observed the olivine-spinel transformation at ~6-14 GPa and 873-1173 K with and without deformation (in uniaxial compression with constant strain rate of 3-5 x 10^{-5} s^{-1}). Stress-strain and transformation-time (strain) curves were simultaneously obtained from time-resolved measurements of two-dimensional X-ray diffraction patterns and X-ray radiography images using monochromatic X-ray (energy 50-60 keV). Overpressures needed for initiating the transformation increased with decreasing temperature from 1.5 GPa and 1173 K to 3.8 GPa at 973 K in the case of no deformation. When the sample was deformed, the overpressures decreased by ~0.5-1 GPa, suggesting the enhancement of spinel nucleation by stress and/or deformation. Stresses in olivine, spinel, and the bulk sample (from stress marker arranged in tandem) were similar at the initial stage, and then spinel becomes dominant deformation phase at around 70% transformation. In these runs conducted at more than 973 K, transformation occurred at grain boundaries of parental phase, and the reaction rims were not formed. On the contrary, larger overpressures than ~5 GPa are needed to cause transformation at lower temperature of 873 K even with deformation, in which we observed faulting across the sample associated with lamellar intracrystalline transformations and micro fracture. The thin intracrysatlline lamellae in olivine crystal developed almost parallel to the main fault and consisted of sub-micron fine-grained materials. This may correspond to transformational faulting as previously observed in germanate olivine at lower pressure conditions of ~5 GPa (Schubnel+, SCI13), however further studies with AE measurements and TEM analysis are needed to understand the detailed process. We did not observe clear evidence for the weakening of bulk sample due to the grain-size reduction as proposed in previous studies.

Keywords: high pressure transformation, deformation experiment, D-DIA, in-situ X-ray observation, Deep Earthquakes

On ductile-to-brittle transition of ice-silica mixtures under compressive loading

*Minami Yasui[1,2], Erland M. Schulson[2], Carl E. Renshaw[2,3], Daniel Iliescu[2], Charles P. Daghlian[4]

1. Department of Planetology, Graduate School of Science, Kobe University, 2. Thayer School of Engineering, Dartmouth College, 3. Department of Earth Sciences, Dartmouth College, 4. Geisel School of Medicine, Dartmouth College

On the bodies in the solar system such as Earth, Mars, and icy satellites, various landforms related to the flow and the fracture of ice-rock mixtures are found; for examples, glaciers on Earth, fretted terrains on Mars, relaxed craters and trough terrains on Europa and Ganymede. To clarify the formation processes and structures of these features, it is necessary to understand the rheological properties of ice-rock mixtures.

Ductile-to-brittle (D/B) transition is one of the most important rheological properties to determine the tectonic style on the bodies, flow features and fracture patterns. The D/B transition of water ice has been studied by some researchers and a theoretical model for the strain rate corresponding to the D/B transition was proposed [Schulson, 1990; Renshaw and Schulson, 2001]. This model indicates that the transitional strain rate depends on ice grain size, temperature, confining pressure, and degree of pre-cracks. However, the D/B transition of ice-rock mixtures has not been studied yet. In this study, we carried out compression experiments on ice-rock mixtures to examine the D/B transition. One of the parameters which is expected to affect the D/B transition of ice-rock mixture is a rock content. So we examined the effect of rock content on D/B transition and compared the experimentally observed transitional strain rates to predictions of the model proposed earlier.

The samples were prepared by mixing ice seeds (diameter < 850 μm) and amorphous silica beads with a diameter of 0.25 μm. To fill spaces and to reduce porosity of sample as soon as possible, the distilled water at 0˚ C was filled. The samples were frozen over a period of one day in a cold room set at -10˚ C. We made samples with silica volume fraction f of 0, 0.06, and 0.18. The sample has a cylindrical shape with a diameter of 30 mm and a height of 30 or 60 mm. We performed unconfined compression experiments under constant strain rate from 10^{-5} to 0.6 s^{-1} in a cold room at Ice Research Laboratory, Dartmouth College. The room temperature was set to be -10˚ C.

The deformation behavior, ductile or brittle, under compressive loading is characterized by the shape of stress-strain curve and by the relationship between peak stress on the stress-strain curve and strain rate. In the case of water ice, the peak stress increased exponentially with increasing strain rate in the ductile regime while it decreased with increasing strain rate in the brittle regime. In the case of ice-silica mixture with f=0.06, the peak stress change with strain rate was similar to that with pure ice (f=0), that is, the peak stress reached a maximum at the D/B transition. However, in the case of ice-silica mixture with f=0.18, the peak stress continued to increase with increasing strain rate. The stress-strain curves for f=0.18 remained ductile-like for all strain rates, so the D/B transition for f=0.18 was expected to be greater than the maximum strain rate (0.6 s^{-1}) explored in this study. Consequently, the transitional strain rates for pure ice and ice-silica mixtures were determined; 10^{-3}-10^{-2} s^{-1} for pure ice, 10^{-2}-10^{-1} s^{-1} for f=0.06 and > 0.6 s^{-1} for f=0.18. We found that the transitional strain rate increased with increasing silica volume fraction.

Finally, we compared the theoretical value predicted from the model by Schulson [1990] to the experimental value. In the case of pure ice, the theoretical transitional strain rate was in good agreement with the measured value. On the other hand, in the case of ice-silica mixtures the theoretical value was larger than the measured value. This might be caused by high sensitivity of the transitional strain rate to the stress exponent n, in the power law relationship between peak stress and strain rate ($d\varepsilon/dt = B\sigma_{peak}^{n}$).

Schulson [1990], Acta Metall. Mater. 38, 1963-1976.
Renshaw and Schulson [2001], Nature 412, 897-900, doi:10.1038/35091045.

Keywords: ductile-to-brittle transition, ice-silica mixtures, silica volume fraction, stress-strain curve, compressive strength

Effect of solid particles and grain boundary on deformation of fine-grained polycrystalline ice

*Tomotaka Saruya[1], Koki Nakajima[1], Wataru Shigeyama[2], Morimasa Takata[1], Tomoyuki Homma[1], Nobuhiko Azuma[1], Kumiko Goto-Azuma[2,3]

1. Nagaoka University of Technology, 2. SOKENDAI (The Graduate University for Advanced Research), 3. National Institute of Polar Research

Behavior of Greenland ice sheet plays a fundamental role in global climate change. Understanding of ice sheet dynamics is important for high-accuracy prediction of sea level rise and ocean circulation variation. Although ice sheet behavior has large spatial-temporal scales, importance of microstructure of polycrystalline ice has been suggested from ice-core analysis (e.g., Faria et al., 2014). Flow law of large-grained polycrystalline ice has been studied by laboratory experiments. However, flow law of ice-sheet ice is complicated by various factors. Cloudy bands, which are localized in the ice sheet cores and contains highly-concentrated impurities, show finer ice grains. Although the interaction between solid particles and ice has been discussed by previous papers (e.g., Rempel and Worster, 1999, Durand et al., 2006), detailed effects in polycrystalline ice and ice core are still uncertain. We have performed mechanical tests and microstructure analysis using artificial ice to investigate the effect of solid particles on flow low of fine-grained polycrystalline ice.
We prepared artificial ice with and without silica-particles (particle size of 0.3 μm and dispersed-amount of 0.1wt%). Powder ice (made by spraying pure water and silica-dispersed water into liquid nitrogen) is compressed for an hour with 70 MPa pressure. Deformation experiments were conducted under constant temperature and pressure with various conditions. Our experimental results clarified the effect of solid particles as follows: 1) grain size of silica-dispersed ice is smaller than that of pure-water ice, 2) strain rate of silica-dispersed ice is larger than that of pure-water ice, 3) minimum strain rate (steady-state creep) was not achieved even with 10%-strain for both pure-water and silica-dispersed ice. Generally, a dislocation creep, which has no dependence on grain-size, dominates the ice deformation, however, our results (grain-size dependence and decreasing strain rate) suggest the possibility of grain boundary effect on the deformation mechanism.
In this presentation, we discuss the deformation mechanism of fine-grained polycrystalline ice from deformation test and microstructure analysis, and the flow of Greenland ice sheet.

Keywords: ice-sheet flow, solid particle

Diffusion studies of water ice and its high-pressure phases: Implications for rheology

*Naoki Noguchi[1], Takuo Okuchi[1]

1. Institute for Planetary Materials, Okayama University

Water ice is a primary constituent of the crusts and mantles of the large icy bodies such as Galilean satellites and Edgeworth-Kuiper belt objects. Understanding rheological properties of water ice including its high pressure phases are essential to understanding the dynamics of the large icy bodies. The real icy crusts and mantle include other constituents such as ammonia, Mg- and Na- sulfates, methane hydrate, and non-water ices. The influence of the sub-constituents on the dynamics is never negligible. The dynamics model based on the unary water system, however, will give some important implications, and be the useful approximation.
Our motivation for the rheological studies of water ice is the first step to understanding the dynamics of the real large icy bodies.The differential stress driving the convections of the icy crust and mantle is very low below 0.01 MPa. The deformation experiments at low-stress conditions are technically difficult. Thus the rheological properties of water ices must be examined by another approach. Newtonian-rheological model is most plausible under such low-stress condition. The Newtonian-rheological properties can be inferred from their diffusivities and the theories of diffusion creep. The ordinary isotope-diffusion method using the mass-spectrometer cannot be applied to the ice diffusion study. To defeat this problem, we have developed the isotope-diffusion method using micro-Raman spectroscopy. First, to conduct the diffusion experiments, the method for the quantitative analysis of isotope tracers using micro-Raman spectroscopy was constructed. The diffusion experiment of poly-crystalline ice I_h under confining pressure was carried out by using this technique, and the grain boundary diffusion coefficient was constrained. Further, we applied this method to the high pressure experiment using diamond anvil cell, and the diffusion coefficients of high-pressure phases were determined. In my presentation, I would like to talk about our efforts to determining the rheological properties of the ices and its high pressure phases through the diffusion studies following a short review for the previous studies. In addition, I will also discuss the condition requires to trigger convection in the large icy bodies based on the results of the diffusion experiments.

Keywords: ice, diffusion, rheology, high pressure, icy bodies

Changes of viscosity and yield stress of montmorillonite-water system with reference to consistency limits

*Koichiro Fujimoto[1], Ryuma Ogura[1]

1. Tokyo Gakugei University

Montmorillonite abundantly exists in the slip zones such as earthquake faults and landslides. Water contents are an important factor for controlling slip behavior, since montmorillonite contains a considerable amount of water molecules compared with other clay minerals. Clay-water system is known to act as a Bingham fluid and we estimated yield stress and Bigham viscosity at different water contents from 100 to 1000 % using a rheometer (Brookfield Rheometer). Starting material is montmorillonite (JCSS-3101; Na-montmorillonite from Tsukinuno, Yamagata Prefecture, NE Japan) provided by Japan Clay Science Society. Yield stress drastically decreases from ca. 20000 Pa (100% water content) to ca. 3000 Pa (600%), and it does not remarkable change at higher water content conditions. Bingham viscosity also large decrease from 1.6 Pa・s (100 % water content) to 0.4 Pa・s (600 %) and then it does not show remarkable change at higher water contents. Thus, there is an inflection point at 600%. The consistency limits of montmorillonite are accepted as ~ 10 %, 54 ~ 98 %, and 290 ~ 710 % for the shrinkage, plastic, and liquid limits, respectively. The inflection point is well correlated to liquid limit of montmorillonite.

Keywords: Montmorillonite-water system, Slip zone, Fault gouge

Effect of humidity and interlayer cation on frictional strength of montmorillonite

*Hiroshi Tetsuka[1], Ikuo Katayama[1], Hiroshi Sakuma[2], Kenji Tamura[2]

1. Department of Earth and Planetary Systems Science, Hiroshima University, 2. National Institute for Materials Science

Smectite has been ubiquitously seen in fault gouge [Ohtani et al., 2000; Schleicher et al., 2006; Kameda et al., 2015] and is characteristic by low frictional coefficient [Summers and Byerlee, 1977; Shimamoto and Logan, 1981]; consequently, it has a key role in fault dynamics [Ikari et al., 2007; Ujiie et al., 2013]. The water content of montmorillonite decreases with increasing depth corresponding to temperature and pressure [Bird, 1984]. And the interlayer cation species of montmorillonite change corresponding to depth [Kameda et al., 2016]. Thus, to more understand fault dynamics, it is necessary to study the effect of hydration on the frictional strength of montmorillonite, which have various interlayer cation spices. However, experimental study for frictional strengths of cation-exchanged montmorillonite under controlled hydration state has rarely reported. Because it is known that the water content of montmorillonite increases with relative humidity, we developed the humidity control system in biaxial friction testing machine and investigated the effect of relative humidity (hydration state) and interlayer cation on frictional strength of montmorillonite. The humidity control system consists of two units, the sample holder (pressure vessel) unit and the vapor generating unit. We controlled both the core holder temperature and the vapor temperature independently, thereby controlled relative humidity. The frictional experiments in this study were performed at five different relative humidity (RH) conditions (10, 30, 50, 70, and 90 %). Na-montmorillonite and Ca-montmorillonite (cation exchanged from Na-montmorillonite with $CaCl_2$ solution) were sheared in this study. In all experiments, the samples were applied normal stress during sliding was kept constant at 10 MPa and sheared at 3 μm/s, and the core holder temperature was kept constant at 95 ˚C. The results of frictional coefficients for both Na- and Ca-montmorillonite decrease with increasing RH. The frictional coefficient of Na-montmorillonite decrease from 0.33 at RH 10 % to 0.062 at RH 90 % and the frictional coefficient of Ca-montmorillonite decrease from 0.25 at RH 10 % to 0.037 at RH 90 %. The frictional coefficients of Na-montmorillonite are larger, compared to Ca-montmorillonite at same RH conditions, which is consistent with Behnsen and Faulkner [2013] using water saturated samples. This trend can be explained by difference of hydration energy, that is, the smaller hydration energy leads closer interlayer distance and stronger bonding between silicate layers [Behnsen and Faulkner, 2013]. There is a negative correlation between water content and frictional strength, which is consistent with previous research [Bird, 1984; Ikari et al., 2007]. For explain the decrease of frictional coefficient with increasing relative humidity, there are two main water weakening mechanisms; (1) the shear strength weakens due to hydration of interlayers and expands distance between layers in montmorillonite [Bird, 1984], (2) the shear strength decrease due to water-film on the particles become thick [Moore and Lockner, 2007]. The changes of interlayer distance with interlayer swelling corresponding to relative humidity are discontinuous at atmospheric pressure [Morodome and Kawamura, 2009], whereas water content of montmorillonite increases continuously with increasing relative humidity [Xu et al., 2000]. From our results that frictional strength decrease continuously with increasing relative humidity, the negative correlation between frictional strength and relative humidity can be explained by mainly interparticle swelling. Our results show hydration state and interlayer cation species are particularly germane to frictional strength. For considering frictional strength at deep underground, an important point to emphasize is that Na-montmorillonite is stronger than Ca-montmorillonite not only at saturated with water [Behnsen and Faulkner, 2013] but also dry state.

Keywords: montmorillonite, hydration, humidity, interlayer cation, frictional strength

Effect of preferred orientation on the frictional strength of montmorillonite gouge

*Hiroshi Sakuma[1], Kenji Kawai[2], Ikuo Katayama[3]

1. National Institute for Materials Science, 2. University of Tokyo, 3. Hiroshima University

Clay minerals have been found in the sliding zones of natural faults and landslides. Most clay minerals are composed by the stacking of 1-nm thick structural layers, and shows large surface specific area. The surface of most clay minerals has high affinity with water and some clay minerals swell at highly humid conditions and in aqueous solutions. Since the presence of interlayer water alters the frictional properties of simulated gouges composed by swelling clay minerals, understanding of the swelling state at various environmental conditions is important for fault and landslides mechanics.
The morphology of clay minerals is plates with large aspect ratio. The preferred orientation of the particles along with the sliding plane can change the frictional properties of gouge [1]. Since the degree of preferred orientation depends on the environment of clay mineral formation [2], frictional properties of simulated gouge having clay minerals should be investigated for various degrees of preferred orientation. Here we measured the shear stress of montmorillonite gouges with two different degrees of preferred orientation under dry conditions.
The degree of the preferred orientation of montmorillonite gouge was evaluated by X-ray diffraction method. To prepare the dry montmorillonite particles without interlayer water, thermal analysis (TG-DTA) was conducted before the shear measurements. Highly oriented montmorillonite gouges shows long dehydration time relative to low orientated montmorillonite gouges. This can be interpreted by the difference of permeability of gouges.
Shear experiments were performed at the normal stress from 5 to 40 MPa. Highly orientated montmorillonite gouges shows high shear stress and strong normal stress dependence compared to the gouges of low orientation. This implies the cohesion force acting between montmorillonite basal planes at dry condition have a large effect on the frictional properties of highly orientated montmorillonite gouges.

References
[1] Wintsch, Chrstoffersen, Kronenberg (1995) *J. Geophys. Res.*, **100**, B7, 13021-13032.
[2] Wenk, Kanitpanyacharoen, Voltolini (2010) *J. Struct. Geol.*, **32**, 478-489.

Keywords: Double shear test, Dependence of normal stress, Hydration, Swelling, Clay minerals

Frictional characteristics of brucite (001) plane on the real contact area

*Hanaya Okuda[1], Kenji Kawai[2], Hiroshi Sakuma[3]

1. Department of Earth and Planetary Environmental Science, The University of Tokyo, 2. Department of Earth and Planetary Science, The University of Tokyo, 3. National Institute for Materials Science

Sheet-structure minerals such as clay minerals are abundant in natural faults. As they are thought to be dominant elements of the slip of faults, it is important to investigate their frictional characteristics. While friction coefficients of general rocks are 0.6-1.0 (Byerlee 1978), sheet-structure minerals have smaller frictional coefficients of 0.2-0.4 (Behnsen and Faulkner 2012). Though this weak friction coefficient is considered to be caused by orientation of relatively weakly bonded (001) plane (Moore and Lockner 2004), no experimental evidence was provided. Recent experiments showed that friction coefficient of single crystal specimens of muscovite was about half of that of polycrystalline muscovite (Kawai et al. 2015), implying that the frictional mechanism of (001) planes is important to explain the low friction of clay gouges. The friction coefficients of sheet-structure minerals were thought to be proportional to the interlayer bonding energy (ILBE) of (001) planes (Moore and Lockner 2004), which is associated with mineral specific electrostatic forces between layers estimated by Giese (1978). However, recent experiments and theoretical calculations showed less relationship between ILBE and friction coefficient (Behnsen and Faulkner 2012; Sakuma and Suehara 2015; Kawai et al. 2015). Hence, it is required to understand a physical process that explains the frictional characteristics of sheet-structure minerals instead of ILBE. Here, we investigate frictional characteristics on real contact area of brucite (001) plane to develop the fundamental physics of the friction between (001) planes. Brucite ($Mg(OH)_2$) is a sheet-structure mineral richly contained in serpentinite often observed in natural faults. The crystal structure is simple and this mineral is suitable for the first principles calculations without high computational cost.

We calculate the potential energy surface under the friction of (001) planes of brucite by using the first principles calculation of electronic structure based on the density functional theory. The normal and friction forces were derived from the potential energy map as the method proposed by Zhong and Tomanek (1989).

Our preliminary results show internal friction coefficient = 0.048 and cohesion stress = 0.371GPa in the sliding direction of <010> on (001) plane.

We will estimate frictional characteristics in any sliding direction on (001) plane and discuss dependence of frictional characteristics on sliding directions. In addition, we will compare frictional characteristics of brucite with those of other sheet-structure minerals such as lizardite, talc, pyrophyllite, and muscovite, investigated by Sakuma et al. (2016) and Kawai et al. (2016) and discuss the difference of frictional characteristics on real contact area among sheet-structure minerals.

Keywords: Sheet-structure minerals, (001) plane, Frictional characteristics, Interlayer bonding energy, The first principles calculation of electronic structure

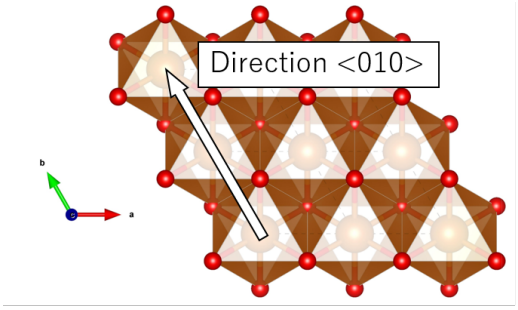

(001) plane

Sliding plane
(parallel to (001)plane)

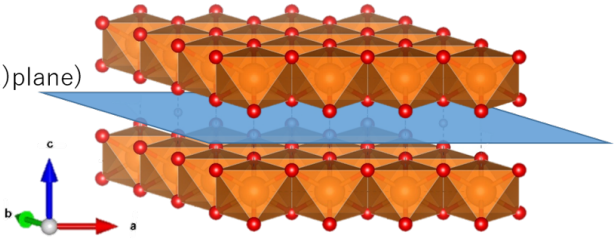

Evolution of the deformation band in the numerical sandbox experiment with 2.4 billion DEM particles

*Mikito Furuichi[1], Daisuke Nishiura[1], Osamu Kuwano[1], Takane Hori[1]

1. Japan Agency for Marine-Earth Science and Technology

We modeled a deformation mechanism of an accretionary prism using the numerical simulation of the sandbox experiment. We solved the motion of 2.4 billion solid particles with Discrete Element Method (DEM) on massively parallel supercomputer system. This huge number of particles enabled us to use the realistic parameters of the sand. Thus, we could successfully reproduce the prism evolution which was consistent with the lab sandbox experiment. One of the advantages of numerical simulation over the analog experiment is the ability to analyze the detailed deformation processes of the granular layer in 3D. We analyzed the mechanical state of particles inside the deformation band to reveal the relations between the growth mode and the wavelength of the deformation. From the results, we discuss the characteristic length to change the deformation mode between the discrete and continuous behaviors.

Keywords: accretionary prism, sandbox, DEM

Scaling of convective velocity in intermittently vibrated granular packing

*NAOKI IIKAWA[1], Mahesh M Bandi[2], Hiroaki Katsuragi[1]

1. Nagoya University , 2. OIST

When a granular packing is mechanically vibrated in a container, convective motion of constituent particles is often induced. This peculiar phenomenon is called ‘granular convection’. Recent studies have suggested that granular convection could occur on the surface of small asteroids such as Itokawa [1,2]. To quantitatively examine the feasibility of asteroidal granular convection, a scaling relation for granular convective velocity has been experimentally developed [3]. However, this scaling relation has been obtained under the steady vibration condition although the actual asteroidal vibration events should be induced by very intermittent meteorite impacts. The scaling relation for convective velocity in an intermittently vibrated granular packing has not been quantitatively obtained so far. Thus, it is necessary to study the granular convective velocity in an intermittently vibrated granular packing. Therefore, in this study, we experimentally measured the granular convective velocity in a two-dimensional granular packing under the successive intermittent vibrations, (tappings). And the obtained velocity scaling is compared with the scaling obtained with a steady vibration.

In the experiment, a two-dimensional chamber filled with bi-disperse disks (diameter: = 10 or 15 mm) is vertically mounted on an electromagnetic vibrator. Then the chamber is subject to 1,000 successive tappings (each tapping event consists of a single period of sinusoidal oscillation). The interval between these tappings is fixed at 2 s. We define the tapping strength Γ as $\Gamma = A(2\pi f)^2/g$, where A is vibration amplitude, f is its frequency, and g is gravitational acceleration (*i. e.* Γ means the ratio of maximum tapping acceleration and gravitational acceleration). Γ is systematically varied as $\Gamma = 2.5, 5, 10, 20$, and f is also varied in the range of $f = 50, 100, 200$ Hz.

In the analysis, we calculated particle velocities using by the particle tracking velocimetry method. In addition, we calculated vorticity field from each particle velocity so that we quantitatively evaluated the occurrence of convective motion in the intermittently tapped granular packing. When the particles form convective motion, we first normalize the mean particle’s velocity v as $v^* = v/(gd)^{1/2}$, where $(gd)^{1/2}$ is the characteristic velocity created by gravity and particle size. We then constructed the scaling relationship between v^* and the dimensionless parameter $S = (2\pi Af)^2/gd$ (Here, S denotes the balance between the squared tapping-velocity and the squared characteristic velocity created by gravity).

As a result, we found a scaling relationship between v^* and S for the intermittently tapped granular packing: $v^* \sim S^{0.56}$ (Fig.1). This result indicates that v is roughly scaled by $S^{1/2}$ which is almost identical to the scaling obtained with a steady vibration. Therefore, we conclude the intermittency of oscillation doesn’t affect the velocity of granular convection.

[1] H. Miyamoto *et al.* , Science **316**, 1011 (2007).
[2] T. M. Yamada *et al.* , Icarus **272**, 165 (2016).
[3] T. M. Yamada and H. Katsuragi, Planet. Space Sci. **100**, 79 (2014).

Keywords: granular convection, scaling, regolith

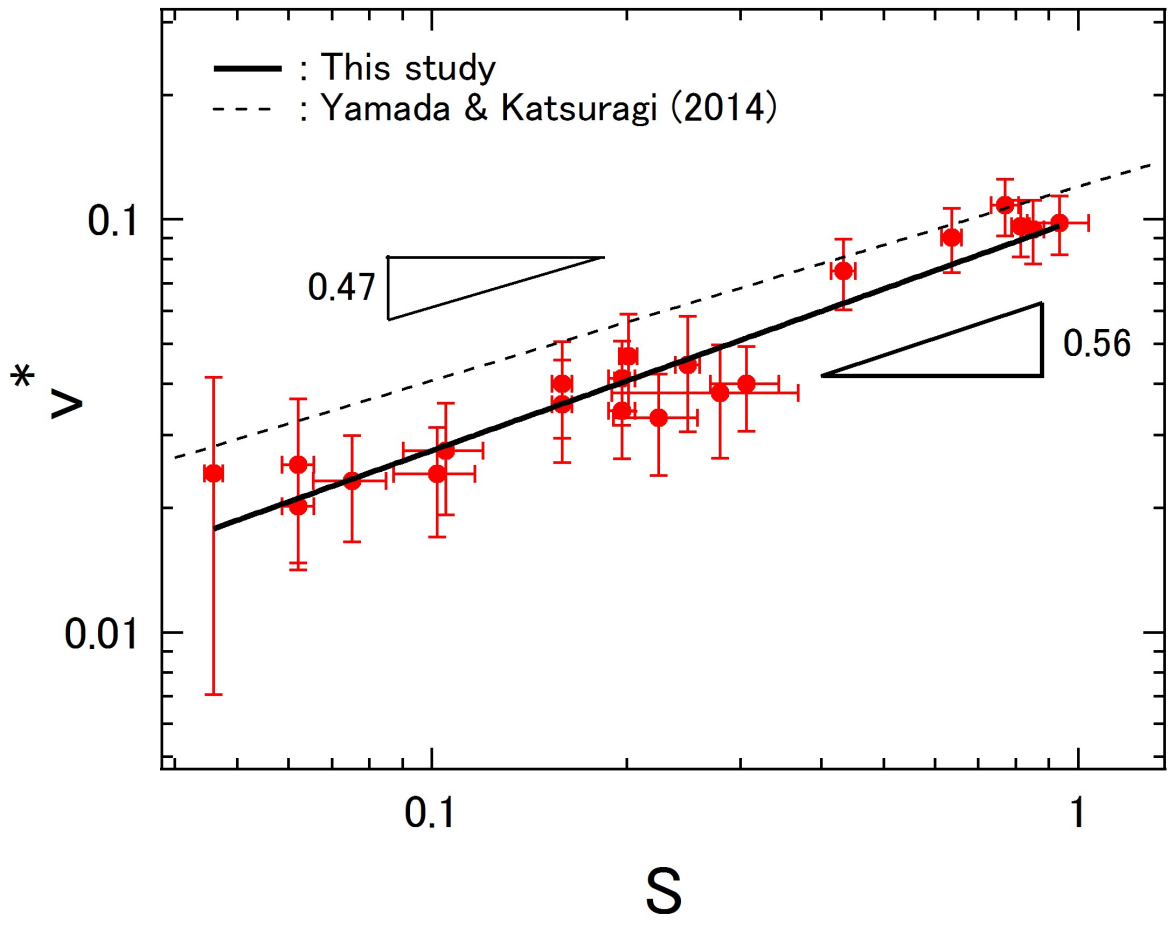

Kinetics study on stress drop and recurrence interval during stick-slip with dehydration

*Masaaki Iwasaki[1], Jun Muto[1], Hiroyuki Nagahama[1], Yuto Sasaki[2]

1. Depertment of Earth Science,Tohoku University, 2. Earthquake Research Institute, University of Tokyo (Graduate School of Science)

It has been found that the phase change of the material and the water generated by dehydration reaction influence the mechanical behavior of the rock. In particular, the frictional stability of the seismogenic zone is considered to change due to friction constant changed by phase-change. Many previous studies focus on instability of slip and localization of strain by the changes in mechanical properties (Proctor and Hirth, 2015). Because the volume of the water generated during the dehydration reaction is generally negligibly small, so that accurate measurement is difficult. For this reason, mechanical behavior is investigated by conducting experiments that controls pore-fluid pressure (Leclere et al., 2016). However, previous study that measures multiple slip events is few. The few studies have been conducted to combine the dehydration with recurrence interval of stick-slip events. In addition, there are few studies that discuss the dehydration not kinetic but mechanical point. In Sawai et al. (2013), kinetic models are applied to describe the dehydration reaction in experiments reproducing the seismogenic zone using serpentinite. Similarly, few studies applied over multiple slip events, and studies have not been conducted on the kinetics of the recurrence interval. When multiple slip events happen with the dehydration reaction, it is possible to describe the recurrence interval in terms of pore-pressure evolution kinetically.
In this study, we analyzed using the data of triaxial compression test made at Sasaki et al. (2016). In the experiment, simulated gouge sample of gypsum hemihydrate, bassanite, between precut gabbro pistons was deformed in high pressure gas medium apparatus at confining pressures of 10 - 200 MPa and temperatures up to 180 ℃. At 200 MPa, 70 ℃ corresponding to non-dehydration condition, samples exhibited stick-slip behavior and the strength of the samples became larger. On the other hand, at 200 MPa, 110 ℃ and higher, likely corresponding to condition for stable anhydrite phase, stick-slip behavior was found to be diminished with the reduction in mechanical strengths with strain.
In this study, we calculate recurrence interval and shear stress drop from data of deformation experiment. We found that recurrence interval and shear stress drop is proportional to confining pressure in experiments with non-dehydration reaction. On the other hand, both recurrence interval and shear stress drop decrease with time despite in an experiment with dehydration reaction. Because the experiment is conducted under constant confining pressure, we consider the decreases in the effective pressure by increasing pore-fluid pressure. From this knowledge, we estimated pore-fluid pressure at time with the effective pressure law. Also, we fit pore-fluid pressure data with Avrami equation. As a result, we found that the evolution of pore-fluid pressure can be described using Avrami equation. From this fact, we consider that by applying the same kinetic approach to different minerals as in this study, it is possible to evaluate the difference of the mechanical properties caused by the dehydration reaction

Asperity contact and constitutive relations in gel friction

*Tetsuo Yamaguchi[1]

1. Graduate school of Engineering, Kyushu University

It is believed that asperity contact plays an important role in fricton, in particular in onset of dynamic slip or stick-slip motions. However, there remain very few studies controling asperities and observing their effects on mascoscopic stick-slip behavior or frictional constitutive laws. Here we perform stick-slip friction experiments between compliant gels with well-controlled asperity shape/size/configurations by molding technique. We find that, as curvature radius of the asperity becomes larger and the normal stress becomes smaller, velocity dependence turns from rate-strengthening to rate-weakening and accordingly, frictional behavior transitions from steady sliding, slow slip to fast slip. In this talk, we discuss the asperity size effects based on microscopic/macroscopic observations as well as a theoretical argument.

Keywords: frictional constitutive relation, stick-slip, slow slip, asperity, laboratory experiment

Rheological variety of mixtures of water and ash collected at Ontake and Sakurajima volcanoes

*Aika Kurokawa[1], Takahiro Miwa[1], Futoshi Nanayama[2]

1. National Research Institute for Earth Science and Disaster Resilience, 2. The National Institute of Advanced Industrial Science and Technology

Most volcanoes are covered with volcanic ash fallen after various types of ash-dominated eruptions. Once the ash combines with water, it is likely to run down slopes. The flow is referred to as lahar, which is widely observed all over the world. Lahar is one of the volcanic phenomena that cause severe damage to surrounding environment, since the speed is generally far faster than that of lava and the onset time is hard to predict [E. Bélizal et al., 2013; S. Jenkins et al., 2015]. Sometimes it occurs just after an eruption [Nakayama and Kuroda, 2003] whereas a large debris flow, which broke out about 30 years after the latest eruption due to heavy rainfall, was reported [Ogiso and Yomogida, 2015]. Moreover, lahar-flow is occasionally accompanied by seismic signals [Walsh et al., 2016; Ogiso and Yomogida, 2015], so that understanding flow characteristics of lahar is important to investigate the relation between lahar-flow and seismicity leading to early detection of the onset in addition to the purpose of simulating the flow.
Based on the background, we have performed rheological measurements of mixtures of volcanic ash and water, which are major compositions of lahar. The volcanic ash used in this study was collected at Sakurajima and Ontake volcanoes in Japan. The reason why the two volcanoes are focused is that lahar had flowed there after recent eruptions although the two types of volcanic ash are apparently different. In order to reveal key features in rheology and to compare rheological characteristics, the viscosity was measured changing the particle concentration and the shear rate. An important point of our findings is that the two types of mixtures show non-linear characteristics differently. For instance, Sakurajima samples show strong shear-thinning regardless of the particle concentration whereas the viscosity fluctuates in a longer time scale than rotational period of rheometer within a certain definite range of shear rate in the case of Ontake samples. Interestingly, the range of shear rate corresponds to that at which the relation between the viscosity and the shear rate shows positive slope or shear-thickening deviating from shear-thinning. Since these non-linear characteristics are considered to be induced by variations in particles such as size and shape [C. Chang and R. Powell, 1994; D. Genovese, 2012; S. Mueller et al., 2014], we mainly discuss the rheological changes of mixtures of volcanic ash and water with consideration for the particle size distribution.

Rheological properties of Izu Oshima lava

*Akio Goto[1]

1. Center for Northeast Asian Studies, Tohoku University

Apparent viscosities were estimated for 1950-1951 and 1986 lava flows effused from summit crater, based on the observed lava flow thickness, lava surface velocity and slope angle (Murauchi, 1950; Minakami, 1951; Shirao, 1986). They ranged 1.7×10^4 Pa s (1063 ˚C) - 3.3×10^6 Pa s (1048 ˚C) in 1950, 5.6×10^2 Pa s (1125 ˚C) - 2.3×10^4 Pa s (1038 ˚C) in 1951 and 1.7×10^4 Pa s - 1.2×10^7 Pa s for LA lava in 1986 (no temperature data). These values are curious in that the viscosity of 1950 lava changed over two orders within 15 ˚C, and 1950 lava at 1048 ˚C had over two orders higher viscosity than 1951 lava at 1938 ˚C. Minakami (1951) also pointed out that the apparent viscosities from observation were several tens times higher than the measured viscosity in laboratory. Systematic study has not been done for Izu Oshima lava rheology thus far. In the present study the viscosity of natural rock samples from Izu Oshima lava, mainly 1986 LC lava, was measured by uniaxial compression viscometry with temperature and stress range between 1000 ˚C and 1100 ˚C and 0.057 MPa and 10 MPa, respectively, at Earthquake Research Institute, University of Tokyo. Cylindrical cores with 15 mm diameter and 30 mm high were used for viscosity measurements. Viscosity was derived from deformation rate and sample dimension using Gent’ s equation (Gent, 1960).

Contrary to the expectation before the experiment that the viscosity decreases continuously with increasing temperature, Izu Oshima lava becomes deformable drastically at around 1100 ˚C. Below this temperature viscosity changes continuously with temperature, although there are over one order scatters among used cores at the same temperature. Their minimum values are 2.1×10^{12} Pa s at 1059 ˚C and 1.7×10^{11} Pa s at 1082 ˚C. These values are almost at solid state and much higher than the observed viscosity. At the temperature that the sample becomes deformable, the main factor of the deformation was not viscous flow but brittle failure. Once the sample started to deform under constant stress, deformation rate increased with time. Or when the constant compression rate was applied, stress decreased drastically with time, which is in contrast with viscous flow that stress goes constant by balancing with applied strain rate. The drastic deformation tended to occur at lower temperature when the applied stress or strain rate was high. The samples after the drastic deformation had vertical cracks on its surface, and in case the compression stroke was large (a few mm) the middle of the cylindrical core was crushed and their surface skin pushed out brittly. Bistered surface gave us doubt that the oxidized strong surface layer sustained the applied stress before the drastic deformation, but the experimental result under reductive atmospheric condition (CO_2+5%H_2) was similar with those done under atmospheric air, indicating the influence of oxidation is minor on the rheological behavior of the used sample.

The present study indicates the Izu Oshima lava was almost at solid state below 1100 ˚C, and above this temperature the main factor of the deformation was not viscous flow but brittle failure. These imply the displacement of Izu Oshima lava was not by Newtonian flow, and these rheological properties may be the source of the above mentioned curious observed viscosity.

Acknowledgements

I am grateful to Prof. Hiraga and his students K. Sueyoshi and K. Yabe for their supports on viscosity measurements. This study is supported by grant in aid for cooperative work from Earthquake Research Institute, University of Tokyo.

Keywords: Izu Oshima, viscosity, rheology

Deformation experiments of foam during solidification -exploring the history of tube pumice-

*Masatoshi Ohashi[1], Mie Ichihara[1], Shiori Takeda[2], Osamu Kuwano[3], Atsushi Toramaru[4]

1. Earthquake Research Institute, the University of Tokyo, 2. Department of Mechanical Systems Engineering, Tokyo University of Agriculture and Technology, 3. Japan Agency for Marine-Earth Science and Technology, 4. Department of Earth and Planetary Sciences, Faculty of Sciences, Kyushu University

Tube pumice is a common product of explosive silicic eruptions forming calderas. It is characterized by bubbles which elongate in one direction. We expect that tube pumice records information about the process leading to a caldera eruption.
In the past, researchers focused on the capillary number ($Ca=R\eta_0\varepsilon'/\Gamma$), which represents the competition between the timescale of shear deformation due to external velocity field and that of shape relaxation due to surface tension. R is the bubble radius, η_0 is the viscosity of the liquid surrounding the bubbles, ε' is the shear rate, and Γ is the surface tension. The more elongated bubbles are observed with the larger Ca in steady states.
However, bubbles deformed by flow may be relaxed if they have enough time in the stress-free condition before solidification of the pumice. We define the pumice number ($Pu=R\eta_0'/\Gamma$) which represents the competition between the timescale of solidification and that of shape relaxation. η_0' is the rate of viscosity increase of the liquid. The elongated bubbles may be preserved in the pumice if the pumice number is high.
In order to determine the effect of the pumice number, we conduct deformation-solidification experiments on polyurethane foam using a rheometer (Ohashi et al., 2016, VSJ fall meeting). Shear strain is applied by rotating the inner rod at a constant speed when the viscosity reaches a specified value. After solidification, we observe the bubble structures of the samples with X-ray computed tomography (CT) and analyze the size and the deformation ratio of bubbles in the 3-D images.
We find a tube-like bubble structure in the sample which experienced large strain. Because it is difficult to quantify the structure due to the limited image analysis technique, experiments are conducted with smaller applied strain. The results clearly show that the deformation ratio cannot be explained by Ca alone. Within a single sample, estimated Ca and Pu vary depending on the sizes and locations of the individual bubbles, and the deformation ratios also vary. For the same Ca, the deformation ratio is smaller for the larger Pu.
To explain the results quantitatively, we apply the time-evolution deformation model with an additional effect of the exponential viscosity increase. The results of numerical calculation show that the amount of the relaxation after the elongation decreases as Pu increases as supposed. However, in the unsteady states, bubbles do not elongate during the shear deformation of the surrounding fluid. The detailed explanation of these behavior will be conducted in the presentation.
In conclusion pumice records bubble elongation at the end of the last shear deformation when Pu is large enough. Tube pumice indicates that the last shear deformation has occurred with sufficiently large Ca and sufficiently large strains.

Keywords: tube pumice, bubble deformation, rheology

Numerical modeling of fracture of porous Maxwell fluid by phase-field method

*Masaharu Kameda[1], Shogo Maruyama[1], Akinori Yamanaka[1], Mie Ichihara[2]

1. Department of Mechanical Systems Engineering, Tokyo University of Agriculture and Technology, 2. Earthquake Research Institute, The University of Tokyo

Brittle fragmentation of vesicular magma is a key process in explosive eruption. Recent estimation on the decompression time in real explosive events indicates that the style of fragmentation is to be “brittle-like fragmentation” (Kameda et al. JVGR 2013), which is defined as the solid-like fracture of the material whose bulk rheological properties is close to fluid state. We also found the fact that the spatial inhomogeneity of bubble distribution is a major source of crack development that may lead to brittle-like fragmentation (Kameda et al. in preparation).
In order to model our findings by numerical approach, we propose a continuum description of fracture in viscoelastic fluid using a phase-field method (Spatschek et al. Phil. Mag. 2011). The phase-field modes with sharp interfaces consist in incorporating a continuous field variable so-called “order parameter,” by which the magma and the bubbles (or the cracks) are distinguished. In this study, the evolution of the order parameter is described using the Allen-Cahn equation consisting of local elastic energy, surface energy and additional numerical parameters. Evolution of crack is driven by local elastic energy. A commercial multiphysics solver (COMSOL) is used as the platform of numerical simulation. The evolution of the order parameter is solved using PDE solver of COMSOL in which weak formulation of the governing equation is described by ourselves. The evolution of strain-stress field in the system is calculated using conventional finite element analysis (FEM) prepared in the solver, in which the rheology of unbroken magma is assumed to be a linear Maxwell fluid.
We consider a sphere consisting of Maxwell fluid and gas bubbles (Fig. 1). In order to reduce the computational cost, one-eighth portion of the sphere is used as the computational domain. A large bubble is placed at the center of the sphere. Another satellite bubble is placed beneath the large bubble. We tested two arrangements about the location of the satellite bubble. In one case, it is placed at the position equal distance away from three planes of symmetry. In another case, the position is biased toward one of the symmetry plane. Physical properties of the materials are determined according to our previous laboratory experiment (Kameda et al. 2013). Isotropic (spherical) negative pressure (gradually increases with time) is loaded outer surface of the computational domain as a decompression.
Time evolution of Maxwell fluid/gas interface is displayed in Fig. 2. Figure 2 indicates that the arrangement of the bubbles remarkably affects the evolution of the crack. The process is divided into four parts: First, a tip is formed on the satellite bubble toward the large bubble. Second, the tip reaches the surface of the large bubble. Third, only in the case where the position of the satellite bubble is biased, a plane crack beneath the large bubble is rapidly developed toward the plane of symmetry. Finally, the plane crack propagates toward outer boundary, then a sharp crack is opened.
We found that stress concentration due to mutual interaction of neighboring bubbles is a dominant factor to evolution of cracks in porous material. Differential stress around a solitary bubble by decompression is inversely proportional to the cube of relative distance in radial direction normalized by its radius (Zhang Nature 1999). In the field of multiple bubbles, the local differential stress is close to the sum of stresses induced by neighboring bubbles. This means that the maximum differential stress is found at the surface of small bubbles close to the large bubble. Evolution of the crack shown in Fig. 2 is explained well with distribution local stress concentration.
In conclusion, this simulation demonstrates that the evolution of crack is very sensitive to the arrangement

of bubbles. Therefore, we should incorporate the effect of bubble arrangement into the criteria for the onset of fragmentation of vesicular magma.

Keywords: Explosive eruption, Fragmentation, Phase-field method

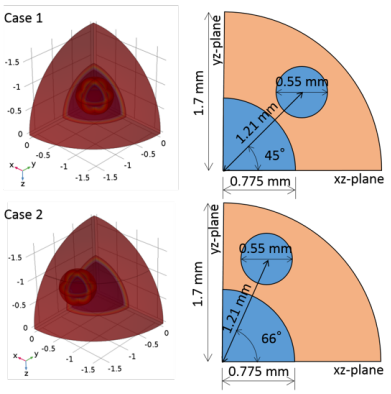

Fig. 1 Bubble arrangement in computational domain

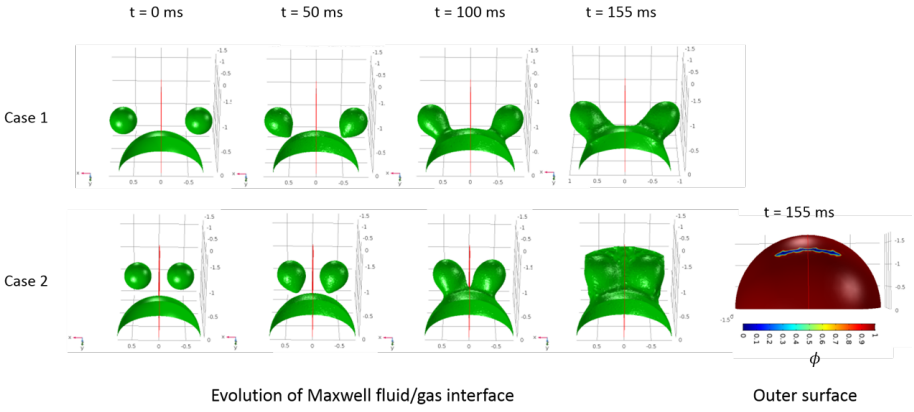

Fig. 2 Crack propagation in porous Maxwell fluid

Chemically induced formation of pull-apart structure of Cr-spinel

Tsubasa Arai[1], Tomoyuki Mizukami[1], Takayoshi Nagaya[2], Simon Wallis[3], Tomoaki Morishita[1], *Yusuke Soda[1]

1. Kanazawa Univ., 2. Tohoku Univ., 3. Nagoya Univ.

Cr-spinel is known as the most rigid mineral among constituents of mantle peridotite. However, it is often seen that it forms pull-apart structures in deformed peridotite as a result of brittle fracturing. Understanding of mechanical conditions for fracturing of Cr-spinel could give a clue for stress estimation. Therefore, comprehensive study on the cause of fractures in Cr-spinel is important. In this study, we performed petrological and microstructural analyses of Cr-spinel and host deformed dunite in Higashi-akaishi ultramafic body in Sanbagawa metamorphic belt. The occurrence can be related to physical and chemical conditions in subduction zones.

Characteristic microstructures of Cr-spinel are developed as a function of an increasing amount of antigorite in the host dunite in the following order: chemical modification from rim to core, pull-apart structures, polycrystalline textures and, finally, disseminated clusters of micro-grains. The microstructural evolution of Cr-spinel implies that there are some chemical effects on the fracturing. The chemical modification of Cr-spinel shows a systematic trend characterized by an increase of Cr# (atomic ratio of Cr / (Al + Cr)) and a subsequent increase of Fe towards end member of magnetite. Extents of chemical modification along cracks are lower than those along rims, indicating that tensile cracks are formed after commencement of chemical modification along rims. The critical mineral chemistry for fractures is defined as $Al / (Cr + Al + Fe^{3+}) < 0.15$. EBSD analyses revealed that sub-grains are dominantly formed in the altered rims and also that tensile cracks are propagated from sub-grain boundaries. Recrystallized micro-grains contain minor sub-grain boundaries and show random orientations, suggesting that they are neoblasts formed by nucleation and growth. The formation of neoblasts is concomitant with Fe-rich parts of Cr-spinel.

The above observations indicate that dislocation-controlled recrystallization depends on chemical compositions of Cr-spinel. Climb velocity of dislocation depends on a self-diffusion coefficient of the slowest diffusing species and self-diffusion coefficient of the slowest Cr in Cr-spinel increases with increasing Cr#. Therefore, it is interpreted that the chemical modification characterized by the increase of Cr# enhanced dislocation motions resulting in the localized sub-grain formation to the chemically modified domains.

We estimated fracture stress (i.e. fracture toughness) of Cr-spinel using a fracture model for a cylinder with a peripheral crack, assuming the widths of chemically modified domains as the potential depths of sub-grain boundaries that act as preexisting cracks. Strength of Cr-spinel is variable depending on mineral chemistry and width of crack and the estimated values for two samples are 84 and 243 MPa. On the other hand, differential stress estimated from dislocation density of olivine is lower than these values. The discrepancy can be explained by concentration of stress due to difference of elastic coefficients of Cr-spinel and surrounding olivine. To support this idea, the maximum intragranular tensile stress in Cr-spinel based on fiber-loading theory is higher than the fracture stress from a cylinder model.

The microstructural analyses reveal that compositional change of Cr-spinel under hydration reactions enhances its plastic deformation to develop weak planar defects such as sub-grain boundaries and grain

boundaries. Fracturing of Cr-spinel can be explained by the chemically induced defects and stress concentration due to the high elastic constant of spinel. It does not require an extremely large stress although the critical strength is variable depending on the Cr# of spinel.

In situ deformation experiments of coesite

*Doi Shunta[1], Yu Nishihara[1], Hirotada Gotou[2], Riko Iizuka-Oku[3], Akio Suzuki[4], Takumi Kikegawa[5]

1. Ehime University GRC, 2. ISSP, University of Tokyo, 3. GCRC, The University of Tokyo, 4. Department of Earth Science,Tohoku University, 5. KEKIMSS

Since continental crust is chemically rich in SiO_2 and contains a large amount of radioisotope compared with bulk upper mantle, flux of subducting continental crust could affect terrestrial thermal history and chemical evolution. This flux is largely determined by viscosity of continental crust. Based on deformation experiments of quartz, Gleason and Tullis (1995) suggested that behavior of continental crust is controlled by frictional sliding and plastic deformation of quartz up to 90 km depth. Coesite is a stable SiO_2 mineral under P-T conditions from 90 to 270 km depth and expected to play a major role in the mechanical behavior of continental crust at this depth. However only one experimental study on viscosity of coesite has been reported (Renner et al., 2001), and pressure condition in the previous study is limited to 4 GPa (120 km depth) because of the limitation of the Griggs type apparatus.

To study rheology of coesite at higher pressures, in situ uni-axial deformation experiments of coesite was conducted using deformation-DIA apparatus “D-CAP” at the synchrotron beamline NE7A, Photon Factory Advanced Ring (PF-AR), National Laboratory for High Energy Accelerator Research Institute (KEK). Water content and microstructure of starting material and deformed sample were determined by Fourier-transform infrared spectrometer (FTIR) and field-emission scanning electron microscope (FE-SEM), respectively. Two types of starting materials were employed. One is polycrystalline quartz with 20 μm grain size and 460 wt ppm H_2O, the other is polycrystalline coesite 10 μm grain size and 10 wt ppm H_2O. A 7 mm cubic (Mg,-Co)O pressure medium was pressurized by WC and cBN anvils with truncated edge length (TEL) of 5 mm. High temperature was generated by a ϕ3.0/2.5 mm graphite heater and temperature was measured using a WRe thermocouples. To remove the initial stress, annealing was performed for an hour at high pressure (quartz was transformed to coesite at this stage) and then uni-axial deformation was done at constant strain rate. Monochromatic X-ray with 50 keV was used for the in situ observation of sample. Radiograph image was taken by YAG phosphor and CCD camera. Two-dimensional diffraction pattern by incident X-ray with dimension of 0.2 ×0.2 mm^2 was obtained using an imaging plate with exposure time of 3-6 min. Strain was determined from sample length on the radiographic image. Differential stress was calculated using equation by Singh et al. (1998) and shear modulus reported by Chen et al. (2015). Pressure was calculated from thermoelastic parameters reported by Angel et al. (2001) and; Galkin et al. (1987). Deformation conditions were temperature of 800 - 1100 ℃, pressure of 3 - 4 GPa, strain rate of 6.7 $\times10^{-6}$ - 1.1 $\times10^{-4}$ s^{-1}. Since, unfortunately, experiments at high pressures were unsuccessful, pressure condition was similar to that in Renner et al. (2001).

Steady state stress was determined for each deformation. Viscosity of coesite in this study shows good agreement with that reported by Renner et al. (2001) except for data at 800℃. The results fitted by constitutive equation, and stress exponent n and activation enthalpy H* were determined to be 2.9±0.5 and 99.5±27.7 kJ/mol, respectively. Renner et al. (2001) reported n and H* of 2.9±0.5 and 261±45 kJ/mol, respectively. The disagreement of these values may be partly due to large errors of the measured stress in both studies.
Ichikawa et al. (2013) reported that 2.2 km^3 /yr of continental crust material can be subducted to 270 km depth based on the numerical simulation using the flow law parameters of Renner et al. (2001). If flow law parameters determined in this study is used, the flux of continental materials would be less because the

smaller n value causes lower viscosity of coesite under natural strain rate of 10^{-12} - 10^{-15} s^{-1}.

Keywords: coesite, in situ, dislocation creep, continental crust

Mechanical properties of ice-silica mixtures: Fracture toughness and elastic moduli

*Minami Yasui[1,2], Erland M. Schulson[2], Carl E. Renshaw[2,3], Daniel Iliescu[2], Charles P. Daghlian[4]

1. Department of Planetology, Graduate School of Science, Kobe University, 2. Thayer School of Engineering, Dartmouth College, 3. Department of Earth Sciences, Dartmouth College, 4. Geisel School of Medicine, Dartmouth College

Ductile-to-brittle (D/B) transition is a key rheological property to determine the tectonic style (flow features and fracture patterns) on the surfaces of icy bodies in the solar system such as Earth, Mars and icy satellites and it has been studied by numerical models, laboratory experiments, and field observations. The theoretical model of D/B transition indicates that the transitional strain rate is controlled by some factors; for example, a power law relationship between stress and strain rate in a ductile behavior, $d\varepsilon/dt = B\sigma^n$ ($d\varepsilon/dt$ is the strain rate and σ is the stress), fracture toughness, and coefficient of friction [Schulson, 1990; Renshaw and Schulson, 2001]. Particularly, fracture toughness is one of the most important factor to determine the critical strain rate corresponding to the D/B transition. The fracture toughness of water ice has been studied by laboratory experiments and depends on temperature, porosity, ice grain size, etc. For example, the K_{Ic} of non-porous fresh water ice is about 100 kPa $m^{1/2}$ at -10˚ C [e.g., Nixon and Schulson, 1987]. The tectonic features found on Mars and icy satellites has a rocky component with various contents in water ice. Thus, the fracture toughness of ice-rock mixtures is important to determine the tectonic style on icy bodies but it remains unclear. In this study, we measured the fracture toughness of ice-rock mixtures and examined the effect of rock content on fracture toughness. Furthermore, we also measured elastic moduli, Young's modulus and Poisson's ratio, which are closely related to fracture toughness.

The samples were prepared by mixing ice seeds with a diameter smaller than 850 μm, amorphous silica beads with a diameter of 0.25 μm, and distilled water at 0˚ C to fill spaces among the ice seeds and/or silica beads. The samples which had a cylindrical shape with a diameter of 30 mm and a height of 60 mm were frozen in a cold room at -10˚ C for more than one day. The specimens for the measurements of fracture toughness were shaped by cutting original cylindrical sample to a rectangular parallelepiped shape and the notch was made by cutting at the center of basal surface. We made samples with silica volume fraction, f, of 0, 0.06, 0.12, 0.18 and 0.34. Fracture toughness was measured using the method of three-point bending in a cold room at -10˚ C at Ice Research Laboratory, Dartmouth College. The elastic moduli were determined by measuring the ultrasonic velocity of both longitudinal and shear waves. After the measurements, the microstructure of recovered specimens were observed using a cryo-SEM.

The fracture toughness, K_{Ic}, for pure ice was 99.8 ±18.5 kPa $m^{1/2}$, close to those of fresh-water ice obtained in previous studies at -10° C [e.g., Nixon & Schulson, 1987]. The values of K_{Ic} for each ice-silica mixture varied more than that of pure ice yet the fracture toughness increased with increasing silica volume fraction and scaled as the square root of silica volume fraction; i.e., $K_{Ic} \propto f^{0.5}$. Young's modulus, Y, increased linearly with increasing silica volume fraction over the range of silica volume fraction explored in this study. On the other hand, Poisson's ratio, ν, of pure ice and ice-silica mixtures were almost the same, irrespective of silica volume fraction. The average value was 0.33, consistent with that of polycrystalline granular ice at -5˚ C [Schulson and Duval, 2009]. Fracture toughness is related to Young's modulus and Poisson's ratio as $K_{Ic}=\sqrt{G_c(Y/1-\nu^2)}$, where G_c is the critical value of the crack-extension force. In our experiments, we found that the increase in fracture toughness with silica volume fraction primarily resulted from the linear increase in Young's modulus with silica volume fraction given assuming the crack-extension force G_c was independent of silica volume fraction over the range of silica volume

fraction explored in this study.

Schulson [1990] Acta Metall. Mater. 38, 1963-1976.
Renshaw and Schulson [2001] Nature 412, 897-900, doi:10.1038/35091045.
Nixon and Schulson [1987] J. Physique, 48, 313-319.
Schulson and Duval [2009] Creep and fracture of ice, Cambridge University Press.

Keywords: fracture toughness, Young's modulus, Poisson's ratio, ice-silica mixtures, silica volume fraction

Experimental study on the flow law of water ice with porosity higher than 50%

*Minami Yabe[1], Masahiko Arakawa[1], Minami Yasui[1]

1. Department of Planetology, Graduate School of Science, Kobe University

Small to middle-sized icy satellites in the solar system (diameter < several hundreds of km) are mainly composed of water ice and rocky debris and they have porosity over a wide range. On these satellites, various landforms caused by tectonic activities are found; for example, impact craters on icy satellites has a shallow depth, compared with those on rocky bodies such as the Moon. The shallow depth is expected to be caused by the difference of viscosity and deformation strength, that is the strength of water ice is smaller than that of rock. Thus, to understand the tectonic activities on small to middle-sized ice satellites, it is necessary to understand the deformation strength of ice-rock mixtures over a wide range of porosity. Flow law is one of the most important rheological properties to understand the formation processes of flow features found on icy bodies. Furthermore. a deformation strength is characterized by a flow law. Yasui and Arakawa (2010) examined the flow law of ice-silica mixtures with silica mass content of 0-50 wt.% and porosity of 0-20% and they reconstructed the flow law by introducing the factors of silica mass content and porosity. In this study, we focused on the effect of porosity over a range of porosity higher than that explored by Yasui and Arakawa (2010). We carried out creep tests of water ice with a porosity higher than 50% and examined the effect of porosity on the flow law of water ice.

The samples were made of ice grains with an average diameter of 20 μm: they were put in a stainless mold of inside diameter 25 mm and then compressed by a piston to control the porosity of 50, 60, and 65%. We performed creep tests under constant stress from 6.6 to 59 kPa in a temperature-controlled box or a cold room at Kobe University. The temperature was set to be -20 or -10˚ C.

In the case of water ice without porosity, the constant strain rate showing beyond a strain of 2% on the creep curve (a relationship between strain and time) was applied to the flow law. However, in the case of our porous water ice, the strain rate continued to decrease with increasing the time even beyond a strain of 2%. This was caused by the compaction during creep test: for example, the porosity of our porous water ice measured before and after the test was changed from ~50 to ~45% at the temperature of -10˚ C. Therefore, we examined the strain rate in increments of a strain of 0.02 over a range of strain from 0.02 to 0.16 on the creep curve to examine the flow law. As a result, the slope of the fitting line on the relationship between strain rate and stress increased with the increase of strain. In this study, we applied the strain rate at a strain of 0.14 on the creep curve to the flow law to examine the effects of porosity and temperature.

The flow law could be expressed as $d\varepsilon/dt=B\sigma^n$, where $d\varepsilon/dt$ is strain rate, σ is stress and B and n are constants. At same temperature, the strain rate increased with the increase of porosity, that is, the constant B exponentially increased with an increase in porosity: for example, the B of the porosity of 50%, 5.3×10^{-11} $s^{-1}(Pa)^{-n}$, was two orders of magnitude smaller than that of 65%, 1.4×10^{-9} $s^{-1}(Pa)^{-n}$. However, the slope of the fitting line became almost constant, irrespective of porosity. This means that the stress exponent n became almost constant, ~0.9, and it was about 1/3 as small as that of water ice without porosity (n~3). In the case of same porosity, the strain rate increased as the temperature became higher while the stress exponent n became almost constant, irrespective of temperature. The B could be expressed by using the activation energy Q as $B=B_0\exp(-Q/RT)$, where T is temperature, R is gas constant and B_0 is constant. The activation energy Q of our porous water ice was about 60 kJ/mol, irrespective of porosity, and it was a little smaller than that of water ice without porosity, 80 kJ/mol (Barnes *et al.*, 1971).

Keywords: flow law, water ice, porosity, creep tests, activation energy, small to middle-sized icy satellites

Effect of pyroxene on the rheological weakening of olivine + orthopyroxene due to phase mixing

*Miki Tasaka[1], Mark E Zimmerman[2], David L Kohlstedt[2]

1. Shimane University, 2. University of Minnesota

To understand the processes involved in rheological weakening due to phase mixing, we conducted torsion experiments on samples composed of iron-rich olivine + and orthopyroxene. Samples with volume fractions of pyroxene of f_{px} = 0.1, 0.3, and 0.4 were deformed in torsion at a temperature of 1200˚C and a confining pressure of 300 MPa using a gas-medium apparatus.
The value of the stress exponent, n, decreases with increasing strain, γ, with the rate of decrease depending on f_{px}. In samples with larger amounts of pyroxene, f_{px} = 0.3 and 0.4, n the stress exponent decreases from n = 3.5 at lower strains of $1 \leq \gamma \leq 3$ to n = 1.7 at higher strains of $24 \leq \gamma \leq 25$. In contrast, for the samples with f_{px} = 0.1, the stress exponent decreases from n = 3.5 at lower strain decreases only to only n = 3.0 at higher strains. In samples with larger f_{px}, the value of p grain size exponent changes from p = 1 at lower strains to p = 3 at higher strains. Furthermore, Hansen *et al*. (2012) observed that n = 4.l and p = 0.7 in samples without pyroxene (f_{px} = 0) regardless of strain. For samples with larger f_{px}, these values of n and p indicate that the deformation mechanism changes with strain, whereas for samples with smaller f_{px} no change in mechanism occurs.
The microstructures in our samples with larger amounts of pyroxene provide insight into the change in deformation mechanism identified from the experimental results. First, elongated olivine and pyroxene grains align sub-parallel to the shear direction with a strong crystallographic preferred orientation (CPO) in samples deformed to lower strains for which n = 3.5. Second, mixtures of small, rounded grains of both phases, with a nearly random CPO develop in samples deformed to higher strains that exhibited a smaller stress exponent and strain weakening. The microstructural development forming well-mixed, fine-grained olivine-pyroxene aggregates can be explained by the diffusivity difference between Si, Me (= Fe or Mg), and O, such that transport of MeO is significantly faster than that of SiO_2. These mechanical and associated microstructural properties provide important constraints for understanding rheological weakening and strain localization in upper mantle rocks.

Keywords: rheological weakening, phase mixing

Quartz microstructures and paleostress estimates in the Sanbagawa metamorphic belt, Central Shikoku, Japan

*Tadamasa Ueda[1], Ichiko Shimizu[1]

1. Department ofEarth and Planetary Science, Graduate School of Science, The University of Tokyo

The paleostress estimates for the ductile region of the Earth’ s crust largely depends on grain size piezometers of quartz. However, it has long been debated whether extrapolation of experimentally determined piezometric relationships to natural conditions is appropriate. Dynamic recrystallization theories predict temperature-dependent relationships between stress and grain size of quartz, but no systematic works have been made to apply the theories to naturally deformed rocks. We measured grain size of quartz in the Sanbagawa metamorphic belt, using electron back-scattered diffraction (EBSD) mapping, and applied a theory-based piezometric relationship. The samples were taken from the Asemi River route, Shikoku Island, Japan. The metamorphic grades increase northward from the chlorite zone through the garnet zone to the biotite zone and then decrease to the garnet zone. Sampling localities cover all these four zones. Except for the sample taken from the lowest metamorphic grade part of the chlorite zone, quartz shows undulatory extinction, subgrain boundaries, and crystallographic preferred orientations. Small quartz grains occur at the rims of coarse grains and sparsely inside the coarse grains. All the obtained grain size distributions were severely right skewed. The mean and the mode values were not well defined in both linear and logarithmic frequency diagrams because these values vary with the cutoff size. Instead, the grain sizes that occupy the largest area fractions were used for the ‘average’ grain size. The grain size of the largest area fraction ranged between ~20 and ~160 microns. Dynamic recrystallization of quartz is likely concurrent with the peak metamorphism, because grain size increases with increasing metamorphic grades. In addition, quartz fabrics show the top-to-west sense of shear in the south, whereas they indicate mainly top-to-east in the north. Previous geothermometric studies using Raman spectra of carbonaceous materials or the disappearance of pumpellyite yielded peak metamorphic temperatures ranging from ~330 to ~570 ˚C. The obtained stresses increase with decreasing metamorphic grades and reach ~100 or ~250 MPa at their maximum under the assumptions of intracrystalline or marginal nucleation models, respectively. The stress estimates with the marginal nucleation model are similar to or slightly lower than stress values calculated from a quartz flow law under assumptions of the possible plate convergence rate, temperature profile, and ranges of the crustal thicknesses of the subduction zone at the timing of the metamorphism.

Keywords: subduction zone, stress, quartz deformation

Monitoring of elastic wave velocity on the cracked granite during shear deformation

*Tatsuro Kubo[1], Atsuko Namiki[2], Ikuo Katayama[1]

1. Department of Earth and Planetary Systems Science Hiroshima University, 2. Graduate School of Integrated Arts and Sciences, Hiroshima University

[Introduction] Changes in elastic wave velocity have a possibility to illuminate physical processes during earthquake rock failure. As elastic wave velocity was affected by propagation and closing of cracks, laboratory study for triaxial compression tests showed increasing elastic wave velocities due to dilation and compaction with increasing confining pressure (Scholz et al. 1973). Seismic observation also showed variations in elastic wave velocity. Li et al. (1998) found that fault-zone p- and s- wave velocities increased with time after 1992 Landers earthquake. To find systematic variations in elastic wave velocity may approach a prediction of failure mode in seismic cycle. In this study, we focus on the detecting of systematic variation in elastic wave under friction experiments, and monitor the change in elastic wave velocity during shear deformation.

[Experimental methods] We conducted monitoring of elastic wave velocity during friction experiments using by biaxial friction machine. Two sliding surface were made by two side blocks placed together to produce a double-direct shear configuration. Normal stress was applied via a hydraulic ram on the side blocks with 5, 10, 20 MPa, and then shear stress was applied by advancing central block downward at constant velocity. Samples we used as simulated host rock were Aji granite. These were thermally cracked with baking at 600 C for 4 hours, because the host rocks along fault zone were expected to have amount of cracks produced by seismogenic faulting movement. In observation of elastic wave velocity, we adopted pulse transmission method using electric transducer directly attached on sample with a direction normal to simulated slide surface sandwiched between these. Elastic wave velocity, amplitude and wave period from waveforms were recorded by oscilloscope.

[Results&Discussion] Observed elastic wave velocity passing through Aji granite samples have a tendency to increase with increasing normal stress due to closure of pre-existing cracks with an orthogonal plane to normal stress. Response in elastic wave velocity given by shear stress showed systematic change similar to that of normal stress, increasing elastic wave velocity with increasing shear stress. This change in elastic wave velocity can be mainly explained by closure of pre-existing cracks with an orthogonal plane to shear stress. The change cannot be observed in phases that shear stress reached at steady-state friction. We also observed change in amplitude during experiments from waveform recorded by oscilloscope. Amplitude increases with increasing normal and shear stress, however amplitude showed almost constant value in phases that shear stress reached at steady-state friction, similar to that of elastic wave velocity. Our results showed that changes in elastic wave velocity and amplitude have a systematical dependence on stress state. As a stress is expected to accumulate in inter-seismic phase in seismic cycle, monitoring a temporal variation in elastic wave velocity and amplitude along fault zone has a one of possibility to understand process of earthquake failure.

Keywords: elastic wave velocity, friction experiment, cracked granite, earthquake hazard assessment

Fractal Size Reduction and Critical Slip Displacement during Fault Slip

*Momoko Hirata[1], Jun Muto[1], Hiroyuki Nagahama[1]

1. Department of Earth Science, Tohoku University

1. Introduction

To evaluate an occurrence of unstable slip, a systematic understanding of frictional instability is necessary. Critical slip displacement has been used to evaluate frictional instability of faults. The critical slip displacement is defined as the slip over which strength breaks down during fault slip or the slip distance, at a constant velocity, through which a population of contacts is destroyed and replaced by an uncorrelated set [Marone and Kilgore, 1994; Scholz, 2002]. Although previous studies have proposed various relationships between critical slip displacement and other factors [e.g., Sammis and Biegel, 1989; Marone and Cox, 1994], it is still open to debate that which factors dictate the critical slip displacement. In this study, we aim to theoretically clarify a factor that determines the critical slip displacement. Additionally, as fractured areas have a self-similar structure, we utilize fractal theory for understanding of the critical slip displacement. Through this study, it is clarified that comminution characterized by the fractal size reduction determines the critical slip displacement.

2. Fractal dimensions with comminution processes

A fractal dimension of surface roughness changes with comminution processes of materials: It takes on the values 3.0, 2.5, and 2.0 from high-velocity impact experiments, conventional milling, and finer grinding, respectively [Hukki, 1962; Rumpf, 1973; Nagahama, 1991, 1993; Muto et al., 2015]. Let us consider the underlying cause of changing in the fractal dimension of surface roughness. When rocks receive external force, a portion of work done externally is used for energy dissipation for fracturing. The energy per unit mass for fracturing is in proportion to the exponential function of a characteristic linear dimension with the fractal dimension of surface roughness as an exponent. Consequently, comminution processes influence the fractal dimension of surface roughness as well as dissipative energy for fracturing.

3. Relationship between critical slip displacement and shear strain

Shear strain for crushing gouge is defined as a ratio of a function related to particle size to shear stress [Draper, 1976]. The function can be approximately expressed as the maximum grain diameters after shearing with the fractal dimension as an exponent. The critical slip displacement is approximately proportional to the final maximum grain size [Dieterich, 1981]. Therefore, the relationship between the critical slip displacement and shear strain can be described as a linear function on a log-log plot. The slope of this function is related to the fractal dimension of the surface roughness. This relationship obtained from theoretical analysis is consistent with previous experimental datasets [Marone and Kilgore, 1993]. Thus, the fractal dimension of the surface roughness controlled determines the critical slip displacement.

4. Discussion –implication of dissipative energy

Fractal size reduction of materials also determined the surface roughness and particle size ranges. Through the theoretical analysis, it is clear that large dissipative energy means small critical slip displacement and/or high fractal dimension of surface roughness. The fractal dimension of the surface roughness ranges from two for smooth surfaces to almost three for rough surfaces [Avnir et al., 1983; Nagahama, 1993]. Thus, small fractal dimension of surface roughness, or small dissipative energy, indicates that gouge particles with various size ranges compose smooth surfaces with filled opening areas.

5. Summary
From this study, it is obvious that the critical slip displacement is originally determined by fractal size reduction of materials. Difference in comminution processes produces the differences in dissipative energy for fracturing, particle size ranges, the surface roughness, and the critical slip displacement.

Keywords: critical slip displacement, dissipative energy, frictional instability , fractal

Mode of tunnel deformations induced by loading in wet granular layer

*Ayuko Shinoda[1], Shin-ichi Fujiwara[2], Hiroaki Katsuragi[1]

1. Graduate School of Environmental Studies, Nagoya University, 2. Museum, Nagoya University

Stable burrows in wet sediments dug by tidal and shore animals play important roles not only in the ecological behaviors of the animals, but also in material circulation in the substrate and the sediment conditions. Thus, the burrow stability problem has been a challenging topic in the fields of sedimentology and biology. Modern ocypodid crabs are known to dig deep burrows in a sandy beach (Seike and Nara, *Palaeogeog., Palaeoclimat., Palaeoecol*, 252 (2007) 458). However, it has not been clarified that how stable these burrow structures are against the external loading.

For the quantitative understanding of strength of a burrow in sandy beach, we modeled it by a tunnel structure in wet granular layer, and focused on mechanical property of wet granular matter. According to the previous works, its mechanical property shows complex behaver. For example, tensile strength of wet granular column nonlinearly depends on liquid content (Scheel et al., *Journal of Physics: Condensed Matter*, 20 (2008) 494236, Herminghaus, *Wet Granular Matter: A Truly Complex Fluid, World Scientific* (2013)). However, little is known about the strength of a tunnel structure formed in wet granular layer.

In this study, we conducted a simple experiment to investigate the mechanical property of a tunnel structure in wet granular layer. In the experiment, we observed how the tunnel structure was deformed by slow uniaxial compression. During the compression, the projected cross section of the deformed tunnel was filmed by a CMOS camera. The compression force was also measured by a testing machine. In this experiment, we mainly varied following parameters: liquid content, packing fraction, initial diameter of the tunnel, and grain size. By analyzing the acquired movies, we examined the temporal evolution of a projected cross section of the tunnel structure. We found that the mode of tunnel deformations can be classified into three types: continuous shrink, shrink with collapse, and subsidence by collapse. The experimental result indicates that the mode of deformations is principally determined by the initial diameter of a tunnel and grain size.

Furthermore, based on a simple model of the force balance for tunnels in soil (Knappett and Craig, Craigs Soil Mechanics, Spon Press (2012)), we estimated the maximum shear stress applied to the tunnel structure. In addition, we defined two types of strengths characterizing a tunnel structure: yield and maximum stresses. As a result, we found that these strengths show qualitatively different dependences on experimental parameters.

Finally, we briefly discussed the condition to maintain a tunnel structure in a sandy beach environment by using the experimental result and information obtained in previous works (Seike, *Marine Biology*, 153, (2007) 1199-1206, Sassa and Watabe, *Report of the Port and Airport Research Institute*, 45, 4,(2006) 61-107).

Dependence of the Constitutive Parameters of RSF Law on Slip Velocity and Temperature at Subseismic Slip Velocities

*Ryuji Nakano[1], Akito Tsutsumi[1]

1. Graduate School of Science, Kyoto University

1. Introduction

The behavior of frictional resistance at intermediate ($10^{-3} < v < 10^{-1}$ ms^{-1}) to high slip velocities ($>10^{-1}$ ms^{-1}) are quite different from that at low slip velocities ($<10^{-3}$ ms^{-1}); at low slip velocities the value of steady-state friction coefficient tends to be between 0.6 and 0.85 [Byerlee, 1978], at intermediate slip velocities steady-state friction resistance exhibits velocity-weakening or velocity-strengthening, and at high slip velocities it shows dramatic velocity-weakening. The cause of this weakening/strengthening behavior is considered to be frictional heating (temperature) during the slip on a fault. For better earthquake prediction, it is required that earthquake simulations considering this behavior are performed. However, previous friction constitutive laws cannot explain the behavior efficiently.

One of the most useful friction constitutive law is rate- and state-dependent friction constitutive law (RSF law), developed by Dieterich [1979] and Ruina [1983]. RSF law was originally described to explain the behavior of frictional resistance at low slip velocities, and it has not been clarified whether this law can also explain the frictional behavior at intermediate to high slip velocities. In addition, the behavior of frictional resistance depends not only on slip velocity but also on temperature, so it is required to clarify the relationship between RSF law and temperature.

In this study, we carried out friction experiments at intermediate to high slip velocities, and estimated the constitutive parameters of RSF law from the experimental results considering the variation of temperature on the frictional surface.

2. Method

We conducted slip velocity step tests using a rotary-shear, intermediate- to high-velocity friction testing machine in Kyoto University at a normal stress of 1.5 MPa under room temperature and room humidity conditions. As a sample, we used a pair of hollow cylindrical Zimbabwe gabbro with an inner/outer diameter of 26/40 mm without sandwiching gouges. For the step, we defined two parameters, IRPM and ΔRPM; IRPM is the value of rotation rate of the servo-motor installed in the machine before stepping, and ΔRPM is one of slip velocity stepping. We selected all the combinations of IRPM and ΔRPM throughout the experiment: a value of IRPM of either 10, 20, 50 or 100 RPM, and a value of ΔRPM of either 80, 150, 200, 300 or 400 RPM. Note that we performed the next combination after the temperature on the frictional surface went down to the room temperature.

To estimate the values of constitutive parameters of RSF law and temperature on the frictional surface, we used the Levenberg-Marquardt method modified by Sakamoto et al. [2005] with a quasi-static spring-slider model and the FEM produced by Kuroda [2005], respectively.

3. Results

As a result of the experiments, the value of steady-state friction coefficient decreases with increasing slip velocity, which is consistent with Tsutsumi and Shimamoto [1997]. In the combination of (IRPM, ΔRPM) = (100, 400) frictional melting could be observed, and obvious slip-strengthening was observed until the molten layer was completely created. This result is also consistent with Hirose and Shimamoto [2005], which mentions that initial melting may act as a stopping mechanism for fault slip.

On constitutive parameters, the trends against slip velocity and temperature are similar; the value of each

constitutive parameter linearly increases with increasing slip velocity/temperature. This trend is consistent with Nakatani [2001] and Nakatani and Scholz [2004]; they suggest that the constitutive parameters a and b have a linear dependence on the absolute temperature. However, our discussion on the relationship between the constitutive parameters and slip velocity/temperature is not enough because temperature on the frictional surface increases with increasing slip velocity. Therefore, it is needed to perform a further experiment in which the dependence of temperature on the constitutive parameters can be divided from that of slip velocity.

Keywords: friction, rate- and state-dependent friction constitutive law , intermediate to high slip velocity, temperature

The effect of decompression-induced crystallization on viscosity of basaltic magma: A case study of Fuji 1707 basaltic magma

*Hidemi Ishibashi[1], Yamato Amano[1]

1. Faculty of Science, Shizuoka University

INTRODUCTION

Basaltic magma shows wide variety of explosive eruption style from mild strombolian to intense plinian. At Fuji volcano, mild strombolian eruption is the most common style of explosive eruption (e.g., 864-866 Jogan eruption). However, intense basaltic plinian eruption occurred at 1707 Hoei eruption. Mechanism of basaltic plinian eruption is not well understood. Plinian scoria of 1707 Hoei eruption is characterized by high abundance of plagioclase microlite (> 30 vol.%); the abundance is higher than that of strombolian scoria of 864-866 Jogan eruption. The fact cannot be explained by the difference of conduit ascent rate alone and suggests that difference of pre-eruptive temperature and/or melt water content may play an important role. In this study, we performed numerical simulation of decompression-induced crystallization to investigate the effect of pre-eruptive conditions on magma viscosity and eruption style of basaltic magma.

METHODS

We used the rhyolite-MELTS program (Gualda et al., 2012) for decompression-induced crystallization simulation. Composition of initial melt is the same as that of basaltic melt of the 1707 Hoei eruption. Plhase equilibrium calculations are repeated with 0.1 MPa step from 150 to 0.1 MPa. During decompression, we keep the conditions of temperature and oxygen fugacity (Ni-NiO buffer) constant, and crystallized phases and bubbles are immediately fractionated. Initial temperature and melt water content conditions vary in the ranges of 1184-1094 deg. C and 0.5-3 wt. %, respectively. At each pressure, melt viscosity is calculated from temperature and composition of melt by the model of Giordano et al. (2008) and relative viscosity is estimated from crystal content by Einstein-Roscoe equation, and magma viscosity is calculated from melt viscosity and relative viscosity.

RESULTS

Melt fraction at 1 atm (F_{1atm}) decreases and onset pressure of decompression-induced crystallization (P_s) increases as initial temperature decreases. F_{1atm} decreases from ca. 92 wt. % at 1189 deg. C to ca. 40 wt. % at 1094 deg. C. The relations between P_s-normalized pressure and F_{1atm}-normalized melt fraction are almost the same for runs of different initial conditions, indication that pressure-melt fraction path of decompression-induced crystallization is chiefly controlled by initial temperature condition. Increasing rates of magma viscosity during decompression strongly depend on initial temperature; magma viscosity is almost constant at 1184 deg. C whereas it increases by 6 orders of magnitude at 1094 deg. C during decompression.

DISCUSSION

Our results indicate that the effect of decompression-induced crystallization on magma viscosity strongly depends on pre-eruptive temperature condition. As initial temperature decreases, increasing rate of microlite increases, and as a result, both melt viscosity and relative viscosity increase. Therefore, magma viscosity significantly increases for initially H_2O-rich low-T basaltic melt. Increase of magma viscosity facilitates fragmentation. In addition, abundant microlites may suppress bubble coalescence and melt-bubble decupling. Consequently, magma degassing is inhibited and explosivity increases. In

conclusion, eruption style of basaltic magma is strongly influenced by pre-eruptive temperature.

Keywords: decompression-induced crystallization, basaltic magma, viscosity, Fuji volcano, MELTS, eruption style

Viscoelasticity and Shear Deformation of Foam during Solidification

*Takeda Shiori[1], Masatoshi Ohashi[2], Osamu Kuwano[3], Masaharu Kameda[1], Mie Ichihara[2]

1. Department of Mechanical Systems Engineering, Tokyo University of Agriculture and Technology, 2. The Earthquake Research Institute, the University of Tokyo, 3. Japan Agency for Marine-Earth Science and Technology

Pumices produced by caldera-forming eruptions have a characteristic structure in which bubbles are elongated in one direction. They are called tube pumices. This study is a part of the research project to elucidate the origin of tube pumices to understand the behavior of magma in caldera-forming eruptions. The research uses rigid polyurethane foam (PUF) as a magma analogue. PUF is porous plastic material generated by mixing polyisocyanate liquid and polyol liquid with catalysts, blowing agents, and/or foam stabilizers. PUF during solidification is viscoelastic, which foams and solidifies like magma during an eruption. Magma is also viscoelastic and its behavior depends on viscosity, gas volume fraction, temperature, and time-scale like strain rate. Viscoelasticity of magma in a vent is crucial to determine the types of volcanic eruptions.

To use PUF as magma analogue, it is necessary to understand the mechanical property of PUF itself. This study is made to quantify the viscoelasticity of PUF during chemical reaction by applying shear deformation in various time-scales. This paper describes the results of comparison between oscillatory deformation behaviors and constant shear-rate behaviors.

The PUF is made of mixing polyisocyanate (Hycel 360P) and polyol (Hycel HW-408 without foam stabilizers), both of which are provided by Toho chemical Industry Co., Ltd.

Viscoelasticity measurements were made with a customized rotating cylinder rheometer (AR 2000ex, TA Instruments). The outer cylinder (polypropylene beaker, diameter: 11.5 mm) is held in place. The inner cylinder (aluminum rod, diameter: 7.5 mm) is controlled by the motor and rotates. The gap of the bottom of cylinders is 8 mm.

The PUF stock solution was poured between the cylinders. It expanded with heat generation to 60% porosity. We recorded temperature of the side of the cylinder by an infrared thermometer. The state of expansion was recorded by a video camera. The length of the specimen touching the inner cylinder was measured in the video images. In the oscillation tests, the complex viscosity was determined by comparing the length, the torque, and the angle of rotation. The apparent viscosity was determined by applying constant shear-rate deformation.

Two types of experiments were performed.

First, we measured the complex viscosity to clarify strain-amplitude dependence by oscillation with an angular frequency of 20 [rad/s]. It was found that the reproducibility of the viscoelasticity measurements was good when the strain amplitude was lower than 0.01.

Second, by giving oscillatory deformation and constant shear-rate deformation alternately to the specimen, the complex viscosity and the apparent viscosity were measured. Most polymers follow Cox-Mertz rule which states that the absolute complex viscosity is equivalent with the apparent viscosity when the angular frequency of the oscillation measurement and the strain rate during constant shear-rate deformation are equal (Marrucci, 1996). In a bubble flow, semi-empirical theory shows Cox-Mertz rule being true. According to Llewellin et al. (2002a), apparent viscosity and absolute complex viscosity depend on dimensionless numbers, which are capillary number Ca ($\propto$ shear rate) and dynamic capillary number Cd ($\propto$ angular frequency). The measurement revealed that, Cox-Mertz rule could not be applied to PUF when Ca is larger than 0.1. As Ca increased, the apparent viscosity became significantly smaller than the absolute complex viscosity.

Decreasing the apparent viscosity with increasing Ca has been understood as the effect of bubble

elongation by shear deformation. However, in this experiment, the apparent viscosity decreases more significantly than the semi-empirical estimate. Because the PUF used in this study has a very large porosity. We think that decreasing the viscosity is the result of larger elongation of bubbles which might be caused by bubbles interaction.

Keywords: foam, complex viscosity, apparent viscosity, capillary number

Large Scale High Precision Sandbox Experiments and Large Scale Numerical Sandbox Experiments - Precursory Signal Preceding to Frontal Thrust Formation

*Osamu Kuwano[1], Daisuke Nishiura[1], Takane Hori[1], Mikito Furuichi[1], Hide Sakaguchi[1]

1. Japan Agency for Marine-Earth Science and Technology

To find out the mechanism of the three-dimensional complex shape formation in sequential thrust and uplift of an accretion prism, we have developed a large-scale high precision sandbox experimental apparatus since 2011. After a number of modifications in the experimental apparatus and experimental procedure, we developed a prototype of the apparatus in 2014. In specimen preparation, the thickness of a sand layer is controlled with the precision of less than single particle size. As a result, we obtained high reproducibility of the thrust formation including its position. With such a well-controlled experimental system, we found the precursory signal prior to thrust formation. To grab and understand the signal, we further improved the apparatus by installing the laser displacement sensor (resolution 0.1 μm, span 800mm), a force sensor, and camera array for surface measurement. In addition to the lab experiments, in which we can observe surface phenomena, we conducted the Discrete Element Method (DEM) simulations of the sandbox experiment. In the DEM simulation, we found similar preceding phenomena. We will discuss the mechanism of these preceding phenomena, comparing the lab experiment and the simulation.

Keywords: precursor, earthquake, sandbox experiment, DEM simulation

Feasibility Study of Morphological Characterization to Comminuted Particles by A Particle Characterization Approach (3)

*Daisuke Sasakura[1], Chihiro Kikuchi[1], Osamu Kuwano[2]

1. Malvern Japan ,Div of Spectris Co.Ltd,., 2. Japan Agency for Marine-Earth Science and Technology

A faults zone contains fine rock powders called gouge that have been ground up by past fault motions. Particle size distribution and particle shape of gouge particles may affect the frictional properties of the fault and reflect the comminution process by the past fault motions. It is well known that particle size distribution (PSD) of fault gouge show power-law distributions. Exponent of this power law is considered to reflect the style and degree of deformation. In this report, we will discuss about the relationship between the PSD and the degree of comminution of model particles by automated particle image analysis and laser diffraction as a particle characterization method.
We did several shear experiments using a rotary shear apparatus with the shear displacement ranges between10mm to 1m. As an automated particle image analysis, Morphologi G3-SE (Malvern Instruments) was used for evaluation of particle size and shape. The observation mode was diascopic mode (Transmittance mode) and a magnification was choose to sufficient to cover 1 to 1,000um. The sample was dispersed with SDU (Sample Dispersion Unit) which attached Morphologi G3-SE. Number of measured particles was over than ten thousand and a parameter filter function on software was used based on shape and pixel number of particle image. We also used a laser diffraction instruments with dry dispersion methods, Mastersizer3000 with Aero unit (Malvern
Instruments) for evaluation of particle size in less than 1um as fine particles.

Keywords: Fault gouge, Particle size, Particls Shape, Comminution, Fractal Distributions

